J Mater Sci: Mater Electron (2022) 33:11017–11024

Structural, magnetic, and electrical properties of Nd-substituted cobalt ferrite

Yu Wang[1,*]

[1] *Guizhou Zhenhua Hongyun Electronics Co., Ltd., Guiyang 550018, China*

Received: 4 January 2022
Accepted: 12 March 2022
Published online: 24 March 2022

© The Author(s), under exclusive licence to Springer Science+Business Media, LLC, part of Springer Nature 2022

ABSTRACT

$CoNd_xFe_{2-x}O_4$ ($0 \le x \le 0.2$) ferrite material with spinel structure was successfully synthesized by the sol–gel self-propagating method. The microstructure and electromagnetic properties of Nd-substituted cobalt ferrite were studied. The study found that the substitution of Nd^{3+} for Fe^{3+} at the B site of ferrite changed the electromagnetic properties of the cobalt ferrite. Among them, when the doping amount $x \ge 0.05$, the second-phase $NdFeO_3$ will be formed. The lattice constant of cobalt ferrite after Nd^{3+} substitution first increases and then reduces. The saturation magnetization of $CoNd_xFe_{2-x}O_4$ ferrite exhibits a linear downward trend and coercivity shows an overall upward trend. In addition, the dielectric constant (ε') has raised from 36.15 (x = 0.00) to 336.9 (x = 0.05). When the substitution amount x = 0.05, the cobalt ferrite has good electromagnetic properties, i.e., Ms = 90.3 emu/g, Hc = 197.2 Oe, and ε' = 336.9. Generally speaking, the substitution of Nd can enhance the electromagnetic properties of cobalt ferrite, which provides reference for obtaining high-performance ferrite by rare earth ions substitution.

1 Introduction

In recent years, because the spinel structure ferrite has excellent properties, such as high saturation magnetization, low dielectric loss, and high resistivity, it has a wide range for applications in electronic information devices, magnetic information storage, sensors, noise filters, and optical devices. Among spinel ferrites, $CoFe_2O_4$ has attracted much attention due to its high coercivity, medium saturation magnetization, excellent chemical stability, and mechanical hardness. These characteristics make $CoFe_2O_4$ become a potential material for recording media [1–5]. In addition, cobalt ferrite materials can also be used in high frequency and power devices, especially electromagnetic interference suppression, phase shifters, circulators, and supercapacitors [6–9].

Studies have found the improvement in the performance of spinel ferrite mainly by the optimization of the preparation process, the dopants of different metal ions, the ion distribution of the tetrahedral and octahedral positions, and the sintering rate [10–12]. Due to the unique 4*f* electron orbitals outside the nucleus of rare earth elements, it couples with the 3*d* orbitals of Fe ions in the spinel ferrite structure to form R-Fe (R stands for rare earth ions), resulting in

Address correspondence to E-mail: yuwang_hy@163.com

https://doi.org/10.1007/s10854-022-08080-5

the electrical and magnetic properties of the ferrite improvement. Therefore, rare earth ions have very special electromagnetic properties. This fact also determines the magnetocrystalline anisotropy of spinel ferrite. This unique electromagnetic performance has aroused the great interest of the majority of researchers, hoping to further improve the magnetic and electrical performance of the ferrite and expand its application range by doping an appropriate amount of rare earth elements into the spinel structure ferrite [13].

Rare earth lanthanides have high resistivity and are excellent electrical insulators. They are widely used to modify the structure and electromagnetic properties of ferrites. Many researchers have studied the effect of rare earth ions La, Sm, Gd, Nd, Tb, Ce, and Y substituted to Fe^{3+} ions. Kumar et al. [14] investigated the replacement of Y^{3+} for Ni ferrite, and the results demonstrated that the replacement Fe^{3+} with a small amount of Y^{3+} ions can enhance the saturation magnetization (*Ms*), coercivity (*Hc*), and resistivity (ρ). According to studies by Rezlescu et al. [15], an insulating intergranular layer will be formed at the grain boundary with Sm^{3+} ion doping NiZn ferrite, which can raise the resistivity of ferrite by restraining the oxidation of Fe^{2+} ions. Ghorbani et al. replaced Fe^{3+} with Yb^{3+} in cobalt ferrite, and the results showed that the coercivity (*Hc*) increased with the amount of substitution [16]. Hossein et al. synthesized $CoSm_xFe_{2-x}O_4$ ferrites by a sol–gel spontaneous combustion method. Studies have shown that with the increase of rare earth ions, the saturation magnetization (*Ms*) of the material decreases and the coercivity increases [17]. Noor et al. synthesized $Co_{1-x}Cd_xFe_2O_4$ (x = 0.0 ~ 1.0, step size 0.1) ferrite samples using ceramic technology. The results showed that all samples maintained the cubic spinel structure after Cd^{2+} doping, and the saturation magnetization (*Ms*) was found to increase first and then decrease with the increase of Cd substitution [18]. Franco et al. synthesized $CoY_xFe_{2-x}O_4$ nanoparticles ($0 \le x \le 0.04$) by combustion reaction method. The influence of Y^{3+} ions on the dielectric performance of Co ferrite was studied, and it was found that ε' increased with the increase of Y^{3+} ion concentration [19]. Reddy et al. studied cerium-doped cobalt ferrite. The results showed that all samples showed cubic spinel phase. In addition, the lattice parameter (a) increases first and then decreases with the increase of Ce content, and *Ms* decreases linearly with the dopant content [20].

Among the cobalt ferrites substituted by different rare earth ions, few researchers have used the sol–gel self-propagating method to synthesize them. In addition, there are few reports on the substitution of rare earth ions Nd^{3+} for cobalt ferrites, and the higher magnetic moment of Nd plays an important role in the magnetoelectric properties of cobalt ferrites. In order to solve some gaps in the current Nd-substituted cobalt ferrite and improve the magnetoelectric properties of cobalt ferrite, we tried to use Nd^{3+} instead of Fe^{3+} to synthesize $CoNd_xFe_{2-x}O_4$ ($0 \le x \le 0.2$) ferrite, and its microstructure, magnetic, and dielectric properties were investigated. It is expected to provide a reference for the replacement of rare earth ions to obtain high-performance ferrites.

2 Experimental procedures

2.1 Preparation of cobalt ferrite

The Nd-substituted cobalt ferrite sample $CoNd_xFe_{2-x}O_4$ ($0 \le x \le 0.2$) was synthesized by the sol–gel spontaneous combustion method. First, the weighed chemical analytical reagents $Fe(NO_3)_3{\cdot}9H_2O$, $Nd(NO_3)_3{\cdot}6H_2O$, and $Co(NO_3)_2{\cdot}6H_2O$ were dissolved in deionized water. Put the prepared nitrate particles into a beaker, add citric acid with a molar ratio of 3:1, then add an appropriate amount of deionized water, and heat it in water at a temperature of 80 °C and stir completely for 3 h. After the mixed solution is cooled, add an appropriate amount of ammonia to keep the pH of the solution at 7. Put the mixed solution into an oven at 80 °C for drying and then externally heat to ignite the xerogel to obtain ferrite powder. Then the ferrite powder and the binder (10% PVA) are thoroughly mixed and pressed into a disc (Φ10 mm × h1.5 mm). Finally, the pressed ferrite samples were kept at 1250 °C for 2 h.

2.2 Properties measurement

The X-ray diffraction pattern (XRD) of the sintered ferrite sample is passed through an X-ray diffractometer model DX-2700 (where the target is Cu and the characteristic wavelength is 0.1541 nm). The cross-sectional micrograph of the cobalt ferrite sample is a Phenom XL scanning electron microscope

(SEM) record. The magnetic properties are gauged by the Lakeshore 7404 Vibrating Sample Magnetometer (VSM) at − 15,000 to + 15,000 Oe. The WK 6500P LCR meter bridge was used to acquire the electrical performance of the cobalt ferrite sample at 100 Hz to 1 MHz.

3 Results and discussion

3.1 Crystal structure properties

The phase structure of $CoNd_xFe_{2-x}O_4$ ferrite sample recorded by X-ray diffractometer (XRD) is shown in Fig. 1. All ferrite samples showed characteristic diffraction peaks of cubic spinel structure. When the replacement amount of Nd^{3+} ion (x) exceeds 0.05, an obvious additional peak appears near the diffraction angle of about $2\theta = 33°$. The phase analysis shows that the second phase generated may be $NdFeO_3$. It may be that Nd^{3+} ions enter the tetrahedral or octahedral gaps in the internal structure of spinel ferrite to form a solid solution. Zhong et al. [21] believed that Nd^{3+} ions with a bigger ion radius (1.07 Å) have a small solid solubility in the spinel structure ferrite. Thus, when the substitution amount of Nd^{3+} ions is too high, free Nd^{3+} ions will react with Fe^{3+} ions and O^{2-} inside the crystal lattice to form $NdFeO_3$.

Figure 2a–e is a cross-sectional photograph of $CoNd_xFe_{2-x}O_4$ ferrite samples observed by a scanning electron microscope (SEM). It can be seen from the SEM image that when it is undoped ($x = 0.00$), the crystal grains of the Co ferrite sample are uniform

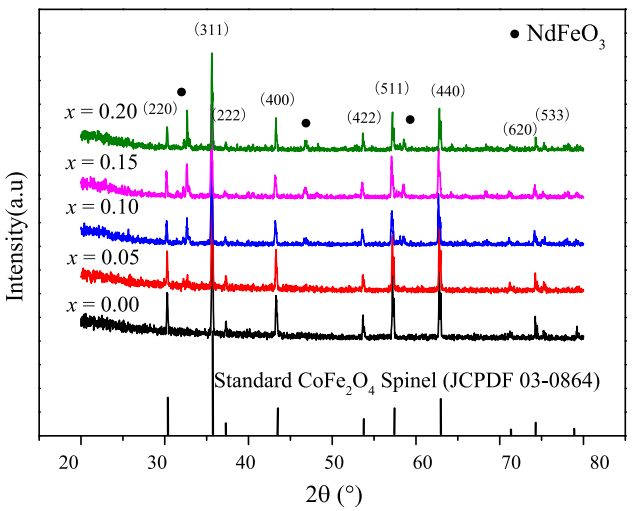

Fig. 1 X-ray diffraction patterns of $CoNd_xFe_{2-x}O_4$ ferrites

and have a good degree of identification. However, the addition of Nd ion leads to abnormal grain growth. And the more the Nd ion substitution, the more serious the abnormal grain growth. This may be because the generation of impurity-phase $NdFeO_3$ hinders the normal growth of Co ferrite grains. Figure 3a–e shows the element content of $CoNd_xFe_{2-x}O_4$ ferrite samples analyzed by an energy-dispersive spectrometer (EDS). From the EDS analysis, it can be known that Nd ions appear when $x \geq 0.05$. Combining the XRD pattern and SEM photos, it can be further confirmed that the impurity phase generated is $NdFeO_3$.

When Nd^{3+} substitution amount $x \leq 0.10$, the lattice parameter of cobalt ferrite gradually expands as the substitution amount increases. This is because the larger Nd^{3+} ion (1.07 Å) in the octahedral structure in the spinel structure replaces the smaller Fe^{3+} ion (0.64 Å) to increase the lattice parameter. With the improve of Nd^{3+} content, the lattice parameter decreases with the increase of the substitution amount, indicating that the cubic spinel phase approaches saturation at $x \geq 0.15$, and the second-phase $NdFeO_3$ precipitates and exists at the grain boundary, which causes the ferrite unit cell to be squeezed. So, the lattice constant of the entire sample shows a downward trend. Table 1 also indicates the crystal and physical parameters of $CoNd_xFe_{2-x}O_4$ ferrite. As the substitution amount of Nd^{3+} ions increases, the porosity of samples enhanced and then declined. It may be because the increase in sintered density is smaller than the improvement in X-ray density (d_x). Therefore, in the light of the porosity formula, $P = (1\text{-}d/dx) \times 100\%$, where d is the sintered density and dx refers to the X-ray density. Among them, the change of sintering density d is because the relative atomic mass of Nd ion (144.2) is greater than that of Fe ion (55.85). In addition, the density of the second-phase $NdFeO_3$ is greater than that of the pure cobalt ferrite, which caused growth in the sintered density of the ferrite samples.

3.2 Magnetic properties

The hysteresis loops of the Nd-substituted $CoNd_xFe_{2-x}O_4$-sintered samples are shown in Fig. 4. After Nd^{3+} replaces Fe^{3+}, the saturation magnetization of $CoNd_xFe_{2-x}O_4$ ferrite shows a linear downward trend. This also indirectly indicates that Nd^{3+} has entered the crystal lattice of the cobalt ferrite sample.

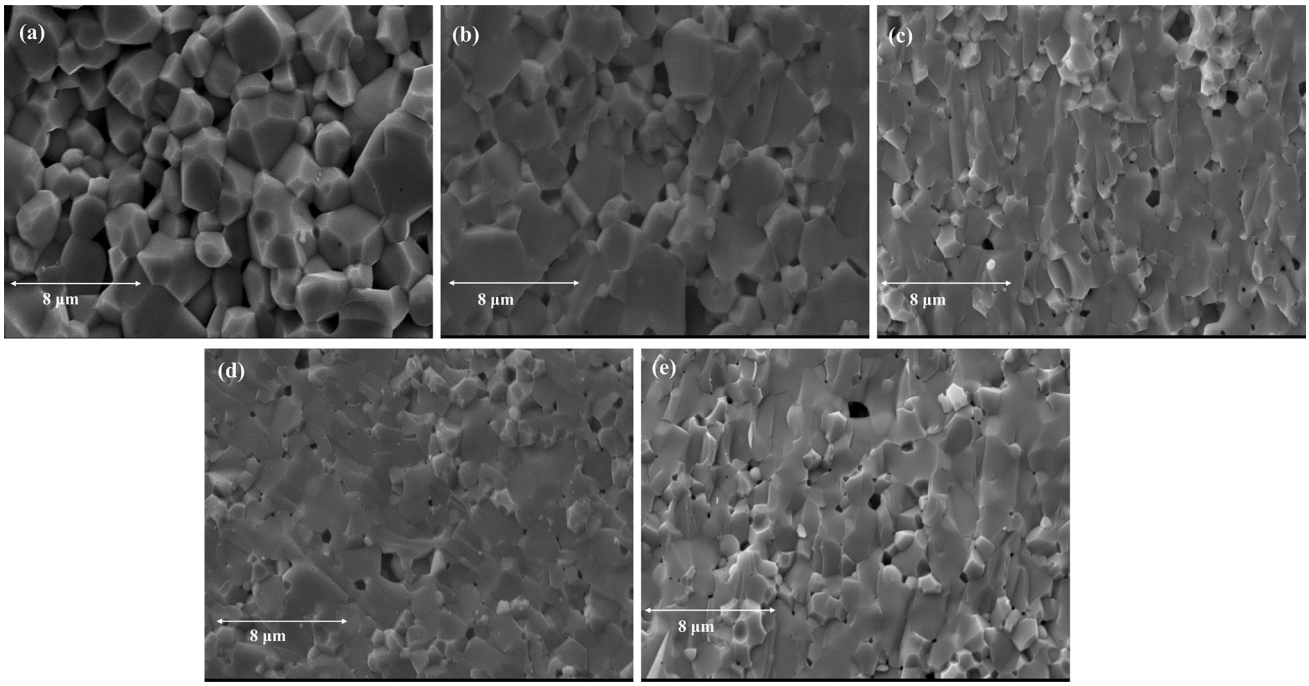

Fig. 2 SEM micrographs of the $CoNd_xFe_{2-x}O_4$ ferrites for **a** $x = 0.00$, **b** $x = 0.05$, **c** $x = 0.10$, **d** $x = 0.15$, and **e** $x = 0.20$

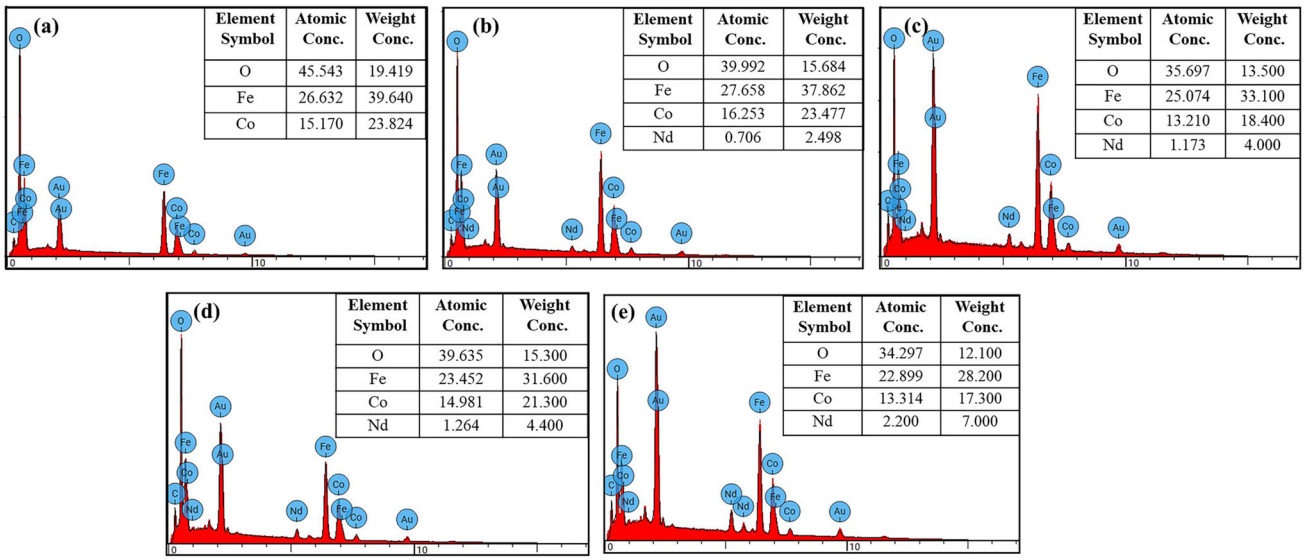

Fig. 3 EDS element map of the $CoNd_xFe_{2-x}O_4$ ferrites for **a** $x = 0.00$, **b** $x = 0.05$, **c** $x = 0.10$, **d** $x = 0.15$, and **e** $x = 0.20$

As we all know, after Nd^{3+} replaces Fe^{3+}, it occupies the octahedral position in the spinel ferrite, resulting in a decrease in the super exchange between A and B and an increase in the negative exchange between B and B. In addition, the magnetic moment of Nd^{3+} ion is 3 μ_B, which is smaller than that of Fe^{3+} ions (5 μ_B) [13]. Therefore, the replacement of cobalt ferrite by Nd^{3+} declines the whole molecular magnetic moment, resulting in a decrease in the saturation

Table 1 Crystallographic and physical parameters of $CoNd_xFe_{2-x}O_4$ ferrites

x	a (Å)	V (Å^3)	dx (g/cm^3)	d (g/cm^3)	P (%)
0.00	8.3586	583.99	5.3392	4.8848	4.8848
0.05	8.3768	587.8	5.4043	5.0697	5.0697
0.10	8.3786	588.18	5.5007	5.2711	5.2711
0.15	8.3768	587.8	5.6041	5.3243	5.3243
0.20	8.3568	583.61	5.7450	5.2973	5.2973

magnetization of the ferrite sample [22, 23]. At the same time, the decrease of *M*s is also related to the impurity-phase $NdFeO_3$. Generally speaking, the pinning influence of the second-phase $NdFeO_3$ at the grain boundary may impede the displacement of the domain wall. Therefore, as the doping content increases, the *M*s of the sample decreases, and the coercive force *H*c presents total upward trend with the increase of Nd^{3+} content. [24]. In addition, the formation of impurity phases results in a lack of uniformity in the resulting sample, which results in improve of shape anisotropy, thereby exhibiting greater coercivity (*H*c).

3.3 Dielectric properties

At room temperature, the real dielectric constant (ε′) changes with frequency (100 Hz–1 MHz) as shown in Fig. 5a. When the frequency is low, the ε′ of pure cobalt ferrite is the lowest 36.15 (x = 0.00) and then ε′ increases with the addition of Nd^{3+} ions. When x = 0.05, the ε′ of the cobalt ferrite sample substituted by Nd reaches the maximum value of 336.9. According to the relaxation ion theory, not all electrons in ferrite can produce electronic transitions. When an external electric field exists, only electrons with a certain kinetic energy can participate in conduction. Even though the low-energy electrons in the crystal lattice do not directly participate in conduction, they will produce local displacement under an external electric field, thereby generating polarization, which helps to increase the ε′. The number of low-energy electrons in $CoNd_xFe_{2-x}O_4$ ferrite determines the real part of the dielectric constant (ε′). In addition, when it is at a high frequency, because the electrons included the polarization inside the ferrite cannot be displaced in time, which caused weakening of polarization and decrease of ε′ value [25–27].

Fe^{2+} ion plays a primary part in the polarization process of the spinel structure ferrite, which is resulted by the electron displacement that locally jumps among Fe^{2+} and Fe^{3+} ions. In addition, the more the Fe^{2+} ions, the greater the dielectric constant and the greater the sensitivity of ferrite to polarization [28, 29]. In the light of Fig. 5a and b, it can be seen that the ε′ of the substituted sample has increased compared to the pure cobalt ferrite sample. May be this phenomenon is resulted by the doping of Nd ions, which reacts with Fe^{3+} ion at the internal grain boundary of the ferrite to form the impurity-phase $NdFeO_3$, thus the number of Fe^{3+}/Fe^{2+} dipoles at the B site in the crystal lattice increases, resulting in a transition in the crystal lattice and the enhancement in the number of electrons increases the real part of the dielectric constant ε′.

Figure 5b displays the rely on the dielectric loss tangent (tanδ) of the $CoNd_xFe_{2-x}O_4$ ferrites tested at room temperature on the frequency (100 Hz to 1 MHz). As we all know, the loss tangent in inhomogeneous dielectric materials is resulted by the polarization hysteresis of the applied alternating electric field [30]. The change of loss curve shows that due to the resistance layer formed by interface polarization and high-frequency polarization hysteresis, tanδ decreases at higher frequencies [31, 32]. Moreover, in the high-frequency stage of low resistivity, because there is less energy between Fe^{2+} and Fe^{3+} ions, there is lower loss. As shown in Fig. 5b, tanδ increases with the increase in the substitution amount of Nd ions. This is because Nd ions enter the internal structure of Co ferrite, which promotes the

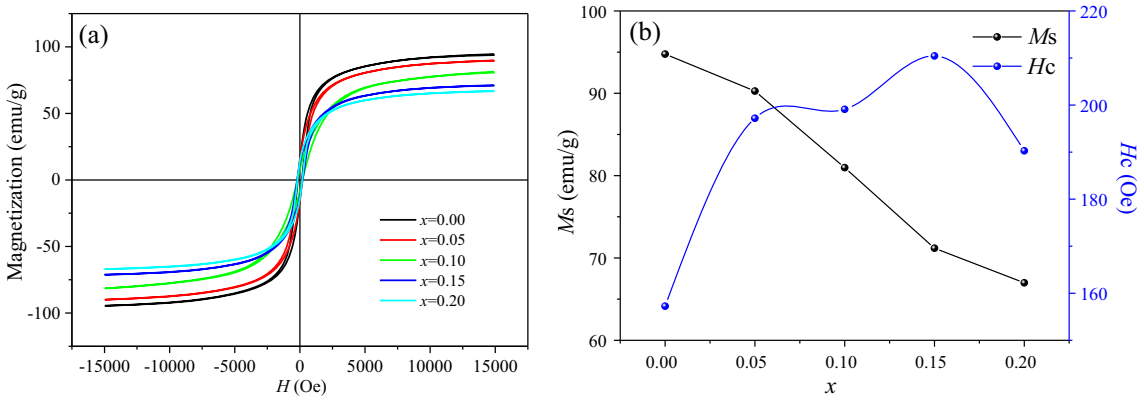

Fig. 4 **a** Hysteresis loops of $CoNd_xFe_{2-x}O_4$ ferrite toroidal rings. **b** Variation trend of *M*s and *H*c values with x for $CoNd_xFe_{2-x}O_4$ ferrites

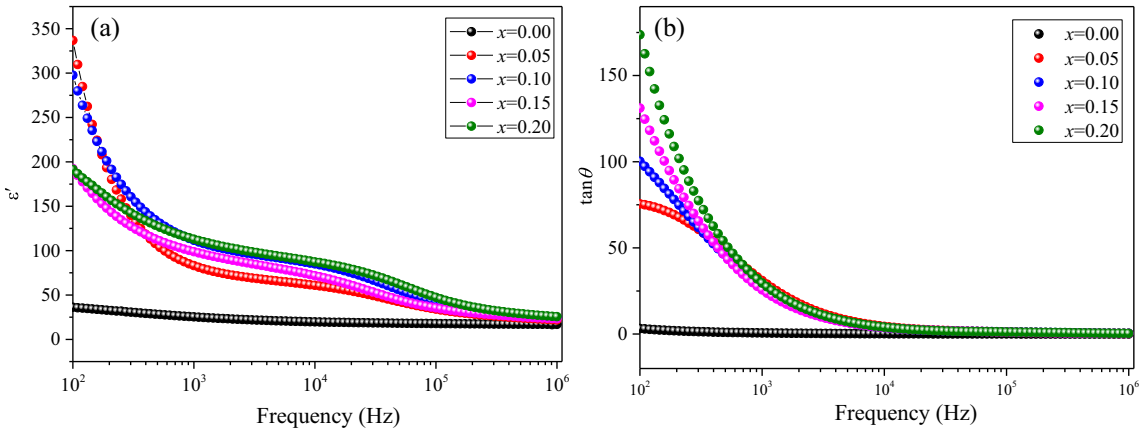

Fig. 5 Electrical properties of ferrites. **a** Frequency dependence of ε′. **b** Dielectric loss tangent spectrum

electronic transition to produce a large amount of Fe^{2+} ions, which enhances the performance of polarization, increases dielectric constant, and high loss.

4 Conclusion

The Nd^{3+}-substituted cobalt ferrite ($CoNd_xFe_{2-x}O_4$) was synthesized by the sol–gel spontaneous combustion method. The results show that the substitution of Nd^{3+} ions for Fe^{3+} improves the lattice constant of cobalt ferrite. This is because Nd^{3+} ions with a bigger ion radius promote lattice distortion and improve the lattice constant of the unit cell. When $x \geq 0.15$, the unit cell is squeezed because of the precipitation of the second-phase $NdFeO_3$, and the lattice constant inclines to reduce. In terms of magnetic properties, the *M*s (saturation magnetization) of the ferrite sample shows a downward trend, and the *H*c (coercivity) shows an upward trend. Due to the doping of Nd^{3+} ions, the real part of the dielectric constant of the cobalt ferrite sample gradually increases, and the tanδ increases with the increase of the doping amount. Nd^{3+} substitution of cobalt ferrite can effectively increase the real part of the dielectric constant ε′ of the sample (from 36.15 to 336.9). When the substitution amount $x = 0.05$, the cobalt ferrite has better magnetic and electrical properties, which provides a consultation for the future production of excellent-performance rare earth elements to replace ferrite.

Author contributions

Author YW contributed to the study conception and design. Material preparation, data collection, and analysis were performed by YW. And the manuscript was written by YW.

Funding

The author declare that no funds, grants, or other support were received during the preparation of this manuscript.

Data availability

All data generated or analyzed during this study are included in this published article.

Declarations

Conflict of interest The author declare that they have no conflict of interest.

Research involving human participants and/or animals This article does not contain any studies with human participants performed by any of the authors.

Informed consent Informed consent was obtained from all individual participants included in the study.

References

1. M.A. Abdo, A.A. El-Daly, Sm-substituted copper-cobalt ferrite nanoparticles: preparation and assessment of structural, magnetic and photocatalytic properties for wastewater treatment applications. J. Alloys Compd. **883**, 160796 (2021)
2. G.L. Jadhav, P.P. Khirade, A.R. Chavan, C.M. Kale, Structural, optical and magnetic properties of diamagnetic cd^{2+} incorporated cobalt ferrite thin films deposited by spray pyrolysis. J. Electron. Mater. **50**, 6525–6534 (2021)
3. B. Ünal, M.A. Almessiere, A.D. Korkmaz, Slimani, Effect of thulium substitution on conductivity and dielectric belongings of nanospinel cobalt ferrite. J. Rare Earths. **38**, 1103–1113 (2020)
4. P. Imanipour, P. Hasani, S. Afshari, M. Sheykh, S. Seifoddini, A. Jahanbani-Ardakani, The effect of divalent ions of zinc and strontium substitution on the structural and magnetic properties on the cobalt site in cobalt ferrite. J. Magn. Magn. Mater. **510**, 166941 (2020)
5. M.M. Rashad, D.A. Rayan, A.O. Turky, M.M. Hessien, Effect of Co^{2+}, and Y^{3+} ions insertion on the microstructure development and magnetic properties of $Ni_{0.5}Zn_{0.5}Fe_2O_4$, powders synthesized using co-precipitation method. J. Magn. Magn. Mater. **374**, 359–366 (2015)
6. R. Valenzuela, Novel application of soft ferrites. Phys. Res. Int. **591839**, 1 (2012)
7. M. Sajjiaa, M. Oubahab, M. Hasanuzzamana, A.G. Olabic, Developments of cobalt ferrite nanoparticles prepared by the sol–gel process. Ceram. Int. **40**, 1147 (2014)
8. J.L. Liu, L.M. Zhang, D.Y. Zang, H.J. Wu, A competitive reaction strategy toward binary metal sulfides for tailoring electromagnetic wave absorption. Adv. Funct. Mater. **31**, 45–2105018 (2021)
9. J.L. Liu, L.M. Zhang, H.J. Wu, Enhancing the low/middle-frequency electromagnetic wave absorption of metal sulfides through f-regulation engineering. Adv. Funct. Mater. (2021). https://doi.org/10.1002/adfm.202110496
10. A.C.F.M. Costa, E. Tortella, M.R. Morelli, R.H.G.A. Kiminami, Synthesis, microstructure and magnetic properties of Ni-Zn ferrites. J. Magn. Magn. Mater. **256**, 174–182 (2003)
11. T.J. Shinde, A.B. Gadkari, P.N. Vasambekar, Saturation magnetization and structural analysis of $Ni_{0.6}Zn_{0.4}Nd_yFe_{2-y}O_4$ by XRD, IR and SEM techniques. J. Magn. Magn. Mater. **21**, 120–124 (2010)
12. F. Ahmed, A. Munir, M. Saqib, Introducing rare earth dopants for controlled conductivity in thermoelectric cobaltites. J. Cond. Magn **28**, 961–964 (2014)
13. Z.Q. Liu, Z.J. Peng, C. Lv, X.L. Fu, Doping effect of Sm^{3+} on magnetic and dielectric properties of Ni-Zn ferrites. Ceram. Int. **43**, 1449–1454 (2016)
14. P. Kumar, G. Rana, G. Dixit, A. Kumar, V. Sharma, K. Sachdev, S. Annapoorni, K. Asokan, Structural, electrical and magnetic properties of dilutely Y doped $NiFe_2O_4$ nanoparticles. J. Alloy. Compd. **685**, 492–497 (2016)
15. N. Rezlescu, E. Rezlescu, Comparative study of the effects of rare earth ions in a high frequency Ni-Zn ferrite. J. Phys. IV. **07**, 225–226 (1997)
16. H. Ghorbani, M. Eshraghi, A.A. Sabouri, P. Dodaran, P. Kameli, S. Protasowicki, Effect of Yb doping on the structural and magnetic properties of cobalt ferrite nanoparticles. Mater. Res. Bull. **147**, 111642 (2022)
17. N. Hossein, J. Elnaz, K. Parviz, G.V. Ali, M. Mohsen, S. Mohsen, Structural features and temperature-dependent magnetic response of cobalt ferrite nanoparticle substituted with rare earth sm^{3+}. J. Magn. Magn. Mater. **543**, 168664 (2022)
18. S. Noor, M.A. Hakim, S.S. Sikder, S. Manjura, K.H. Maria, Magnetic behavior of Cd^{2+} substituted cobalt ferrites. J. Phys. Chem. Solids **73**, 227–231 (2012)
19. A. Franco, H.V.S. Pessoni, Enhanced dielectric permittivity on yttrium doped cobalt ferrite nanoparticles. Mater. Lett. **208**, 115–117 (2017)
20. M.V. Reddy, T.V. Jayaraman, N.D. Patil, Dibakar, Giant magnetoelastic properties in Ce-substituted and magnetic field processed cobalt ferrite. J. Alloys Compd **837**, 155501 (2020)
21. Z.C. Zhong, L.Z. Li, X.H. Wu, X.X. Zhong, Z.X. Tao, H.S. Guo, Influence of Nd substitution on the structural, magnetic and electrical properties of NiZnCo ferrites. Ceram. Int. **47**, 8781–8786 (2021)
22. J. Sun, J. Li, G. Sun, Effects of La2O3, and Gd2O3, on some properties of Ni-Zn ferrite. J. Magn. Magn. Mater. **250**, 20–24 (2002)
23. G.L. Sun, J.B. Li, J.J. Sun, X.Z. Yang, The influences of Zn^{2+} and some rare-earth ions on the magnetic properties of Nickel-Zinc ferrites. J. Magn. Magn. Mater. **281**, 173–177 (2004)
24. Z.J. Peng, X.L. Fu, H.L. Ge, Z.Q. Fu, C.B. Wang, L.H. Qi, H.Z. Miao, Effffect of Pr^{3+} doping on magnetic and dielectric properties of Ni-Zn ferrites by one-step synthesis. J. Magn. Magn. Mater. **323**, 2513–2518 (2011)
25. M.V.S. Kumar, G.J. Shankarmurthy, E. Melagiriyappa, K.K. Nagaraja, H.S. Jayana, M.P. Telenkov, Structural and complex impedance properties of Zn2+ substituted nickel ferrite prepared via low-temperature citrate gel auto-combustion method. J. Mater. Sci: Mater. Electron. **29**, 12795–12803 (2018)
26. A. Thakur, P. Thakur, J.H. Hsu, Enhancement in dielectric and magnetic properties of In^{3+} substituted Ni-Zn nano-ferrites by coprecipitation method. IEEE Trans. Magn. **47**, 4336–4339 (2011)

27. N. Sivakumar, A. Narayanasamy, B. Jeyadevan, J. Joseyphus, Dielectric relaxation behaviour of nanostructured Mn–Zn ferrite. J. Phys. D. Appl. Phys. **41**, 245001–245006 (2008)
28. Q. Li, Y. Wang, C. Chang, Study of Cu Co, Mn and La doped NiZn ferrite nanorods synthesized by the coprecipitation method. J. Alloys Compd. **505**, 523–526 (2010)
29. M. Naeem, N.A. Shah, I.H. Gul, A. Maqsood, Structural, electrical and magnetic characterization of Ni-Mg spinel ferrites. J. Alloys Compd. **487**, 739–743 (2009)
30. M. Azizar Rahman, A.K.M. Akther Hossain, Electrical transport properties of Mn–Ni–Zn ferrite using complex impedance spectroscopy. Phys. Scr. **89**, 25803 (2014)
31. H.S.M. Rahimi, P. Kamelii, M. Ranjbar, H. Hajihashemi, The effect of zinc doping on the structural and magnetic properties of $Ni_{1-x}Zn_xFe_2O_4$. J. Mater. Sci. **48**, 2969–2976 (2013)
32. H.S. Guo, L.Z. Li, X.H. Wu, Z.C. Zhong, Z.X. Tao, F.H. Wang, T. Wang, Enhanced of the resonant frequency of NiZnCo ferrites induced by substitution of Fe ions with Gd ions. J. Magn. Magn. Mater. **538**, 168249 (2021)

Publisher's Note Springer Nature remains neutral with regard to jurisdictional claims in published maps and institutional affiliations.